Observations of the Tasman Front

JOHN C. ANDREWS

Australian Institute of Marine Science, Cape Ferguson, Townsville, Queensland, Australia

MARTIN W. LAWRENCE AND CARL S. NILSSON

R.A.N. Research Laboratory, Edgecliffe, N.S.W., Australia

(Manuscript received 3 January 1980, in final form 15 July 1980)

ABSTRACT

Ship and air surveys were conducted in 1978–79 to examine the thermal structure in and near the Tasman Front between Australia and New Zealand at latitudes between Brisbane and Bass Strait. After separation from the continental slope, the East Australian Current feeds into the conjunction of the warm South Coral and cool Tasman Seas. This conjunction is seen as an abrupt change of temperature at all depths peaking at ~6°C between 150 and 300 m depth. Extreme north-south excursions of the Tasman Front occur and waters of the Tasman or South Coral Sea origin follow the distortions to form equatorward cyclonic meanders or poleward anticyclonic meanders, respectively. These meanders occupy a latitude span of about 400–700 km and form a wave pattern stretching coherently across the Tasman Sea with a wavelength of ~370 km; the average fall in surface dynamic height across the span is 30 cm. Eddy intensification near the Tasman Front produces very large transports but this is mostly recirculating, so in the time-averaged sense only $\sim 15 \times 10^6$ m^3 s^{-1} flows east into the southern limb of the South Pacific subtropical gyre. The abrupt change in the shape and temperature of the thermocline in crossing the Front reinforces Warren's (1970) argument that a zonal jet is maintained near latitude 34°S by baroclinic adjustment in order to connect the western boundary currents which flow along Australia and New Zealand; this composite boundary current is required to close the interior (Sverdrup) wind-driven circulation in the South Pacific. Ship and satellite infrared measurements show that in addition to there being an abrupt change in surface temperature at the Front, the East Australian Current advects very warm water from the north, down the coast and out along the Tasman Front.

1. Introduction

The question of what happens to the East Australian Current after continental separation has been addressed by several authors beginning with Wyrtki (1962) who postulated a broad zonal flow of ~500 km width was fed by the East Australian Current and crossed the Tasman Sea at latitude 35°S. More recently Stanton (1975, 1976) and Denham and Crook (1976) have studied a narrow meandering zonal current frequently found between North Island of New Zealand and Norfolk Island which Denham and Crook named the Tasman Front. This current is structurally similar to the East Australian Current, though much weaker, and this led both Stanton and Denham and Crook to support Warren's (1970) contention that a zonal jet is the most theoretically plausible current system across the Tasman Sea.

The evidence for such a current has been collected mainly close to the Australian and New Zealand mainlands, with very little data taken more than 550 km beyond the continental shelves. The central Tasman Sea has been neglected largely because of the limited endurance of the research ships involved; there have been several cruises which crossed the Tasman Sea but no extensive grid searches were conducted in the central Tasman Sea.

In this paper we discuss the results of large-scale surveys using ships and aircraft near latitudes where the zonal jet (or Tasman Front) should exist. The surveys extended midway across the Tasman Sea and in one case as far as New Zealand. Broadly speaking, the main result is that the conjunction of the warm water from the South Coral Sea and the cool water from the Tasman Sea is seen as a very abrupt thermal front at all depths. The associated pressure gradient gives rise to very swift currents along the Tasman Front toward New Zealand. Gross meridional distortions of the Front occur and water of South Coral or Tasman Sea origin breaks through the Front to form warm core eddies in the Tasman sea or cold core eddies in the South Coral Sea, respectively.

2. The experiments and data analysis

A Royal Australian Air Force Orion aircraft deployed air expendable bathythermograph (AXBT) probes at the positions shown by the filled circles

0022-3670/80/111854-16$08.00
© 1980 American Meteorological Society

on Fig. 1a on 29 August 1978. A course for HMAS *Diamantina* was then chosen to investigate features revealed by the AXBT survey. This track (4–11 September 1978) is shown as the dashed line on Fig. 1a. Expendable bathythermograph (XBT) probes were released at intervals of ~20 km and surface water was continuously sampled with a thermograph. The open circles on Fig. 1a show positions where XBT probes were released from HMAS *Diamantina* during 13–18 September to extend the earlier coverage.

No ships were used during the second experiment (13 December 1978) when a RAAF Orion deployed AXBT probes at the positions shown by the filled circles on Fig. 1b.

Fig. 1c represents the third experiment. The dashed line shows the track of HMAS *Kimbla* (11–19 February 1979) where a geomagnetic electrokinetograph (GEK) was used to obtain ocean current vectors at intervals of ~30 km, interleaved with similarly spaced XBT's and in conjunction with continuous surface thermograph data. This track was chosen to investigate features revealed by AXBT's deployed at the positions marked by filled circles on Fig. 1c from a RAAF Orion on 8 February 1979.

The fourth and final experiment was a ship survey (HMAS *Diamantina*, 22 February–1 March 1979 and 8–12 March 1979) along the tracks shown in Fig. 1d. A continuous surface thermograph recording was made and XBT probes were released approximately every 20 km. Ocean current vector measurements (GEK) were interleaved with XBT measurements.

The standard display for AXBT traces was not used since the resolution is poor; instead a frequency-to-voltage converter was used with a battery-driven strip-chart voltmeter in order to expand the temperature scale to 2.0°C cm^{-1}. Dynamic height anomaly (0/1300 db) was calculated for each bathythermal profile by first calculating the anomaly over the sampled pressure interval from the temperature profile and historical temperature-salinity curves; second, a correction for the remaining pressure interval to 1300 db was obtained from regression relations between deep temperatures and dynamic height. This method was adapted from Andrews's (1976) treatment of West Australian Current XBT profiles. The AXBT's measured to 350 m while some XBT's measured to 450 m and others to 750 m. As an example, if $D(z_1/z_2)$ is the dynamic height anomaly [geodynamic centimeters (gdcm)] over the pressure interval from z_1 to z_2 and $T(z)$ is the temperature (°C) at depth z, the relation we used for standard 450 m XBT's was

$$D(0/1300) = D(0/450) + 3.71T(450) + 53.15. \quad (1)$$

Contour diagrams of $D(0/1300)$ for the four experiments are shown in Figs. 1a–1d. Dashed lines are drawn where we consider that even though there are insufficient data, isopleths are required to produce a consistent or complete picture. The 190 gdcm contours in Figs. 1 are heavily drawn to represent the position of the center of the Tasman Front. This height contour frequently, though not always, coincides with the position of the fastest flowing surface water in the central and western Tasman and South Coral Seas.

The XBT traces were digitized at integral Celsius values, at flexure points, and at 0, 150, 250 and 450 m. Some examples of reconstituted XBT profiles are shown in Figs. 2a–2c but the main displays of vertical structure are vertical isotherm sections to 450 m depth as functions of progressive distances along ships' tracks. These were computer-generated from the digitized XBT data. Thus, Fig. 3a is the section along track BCD of Fig. 1a, Fig. 3b is along EF of Fig. 1a, and Fig. 3c is along GHIJKL of Fig. 1c. Surface temperatures obtained from the thermograph traces are plotted above the isotherm sections to allow the eye to correlate surface fronts with deeper baroclinic thermal fronts. A complete surface isotherm map obtained from all the thermograph data taken during experiment 4 on HMAS *Diamantina* is shown in Fig. 4.

3. Dynamic topographies, currents and transports

Fig. 1 shows that the Tasman Front is a zonal band separating a high-pressure region in the north from a low-pressure region in the south. The band is created by a collection of cyclonic deformations protruding northward and anticyclonic deformations protruding southward so that the Tasman Front takes on more the nature of a planetary wave along a latitude parallel. In fact, Figs. 1b and 1c each contain a full wavelength with southward currents near the coast and out to sea, connected by a northward return flow. Fig. 1d contains one and one-half wavelengths along 34°S, while Fig. 1a shows two full wavelengths out to 163°E, and suggests at least four wavelengths between Australia and North Island. The square on Fig. 1a shows the region where Stanton (1976) found a wavelike meandering zonal jet. It had essentially the same shape and dimensions as the meanders we have drawn between 165°E and North Island. There can be little doubt that the Tasman Front, as its name implies, extends from Australia to New Zealand between the South Coral Sea and the Tasman Sea. Consideration of thermal structure in the next section shows that the Front is in fact an interface between the cool water of the Tasman Sea and the warm water of the South Coral Sea.

Geostrophic and GEK currents are quite swift even as far east as Lord Howe Island (159°E). For

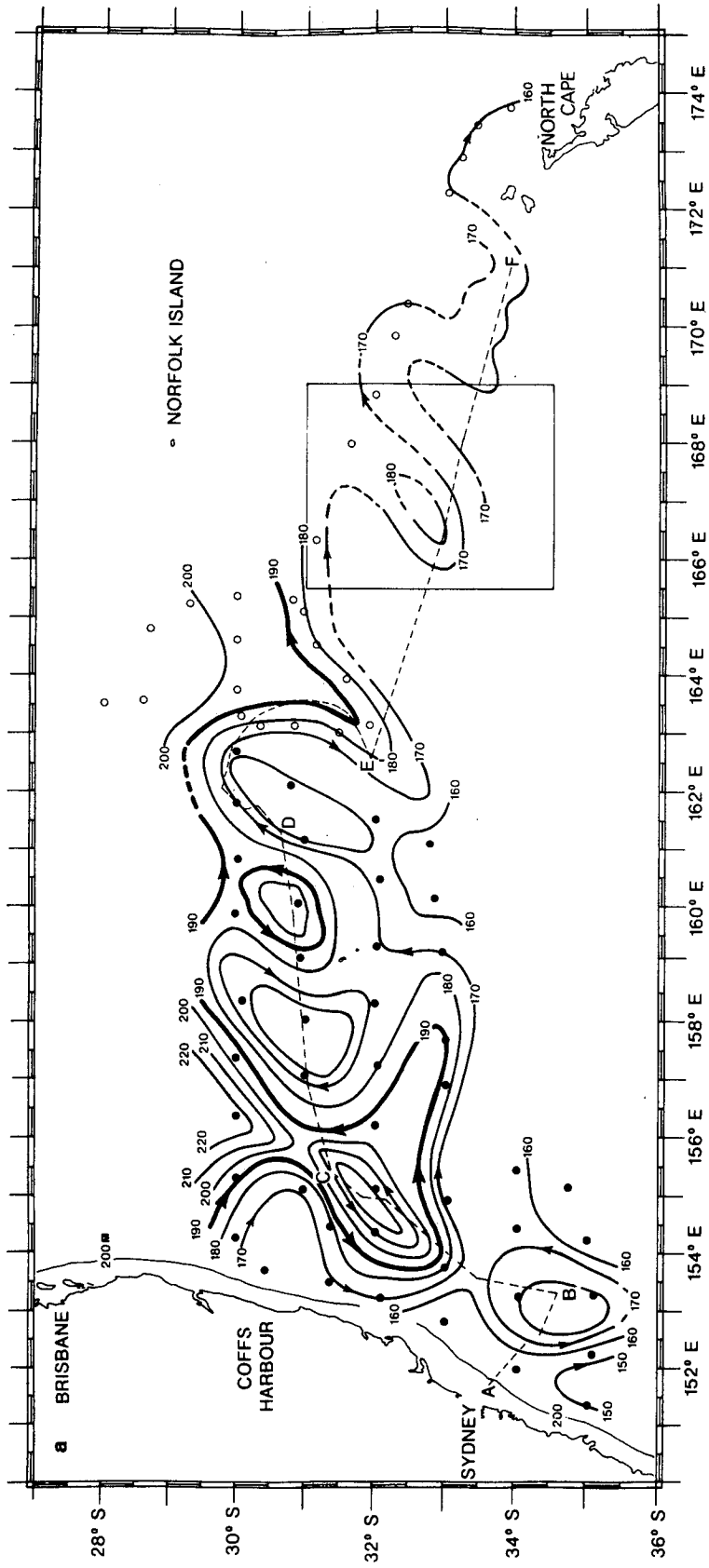

FIG. 1a. Dynamic height anomaly [0/1300 db (units gdcm)] deduced from AXBT probes (29 August 78, filled circles), XBT probes along ABCDEF (HMAS *Diamantina*, 4–11 September 78) and at open circles (HMAS *Diamantina*, 13–18 September 78). The rectangle shows the location of the Tasman Front found by Stanton (1976).

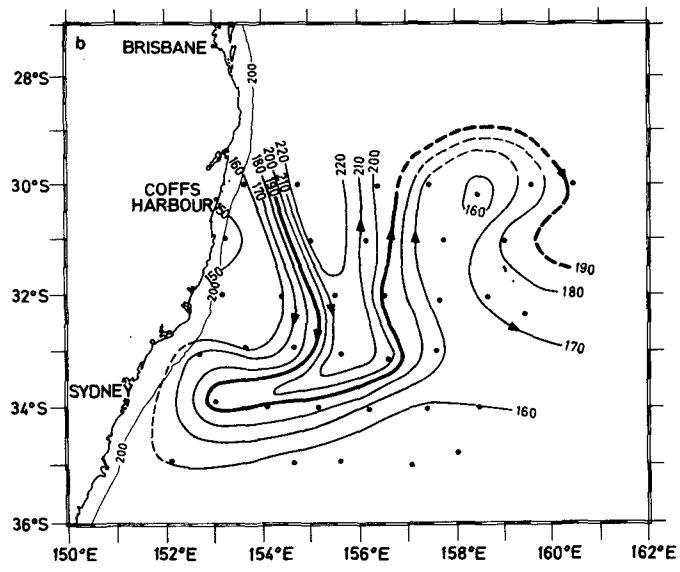

FIG. 1b. As in Fig. 1a except from AXBT probes (13 December 78, filled circles).

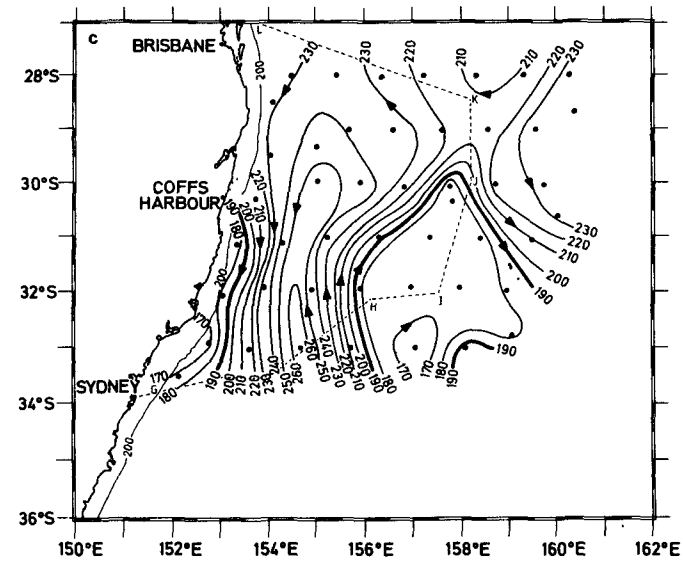

FIG. 1c. As in Fig. 1a except from AXBT probes (8 February 79, filled circles) and XBT probes along GHIJKL (HMAS *Kimbla*, 11–19 February 79).

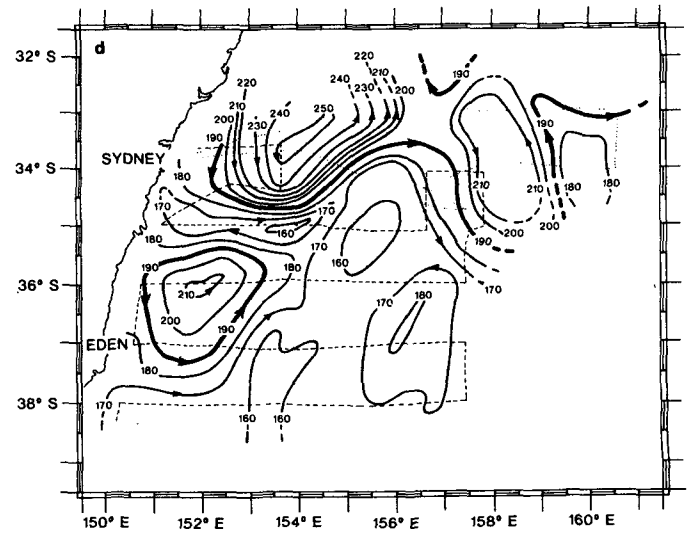

FIG. 1d. As in Fig. 1a except from XBT probes along the track of HMAS *Diamantina* (dashed 22 February–1 March 79; dotted 8–12 March 79).

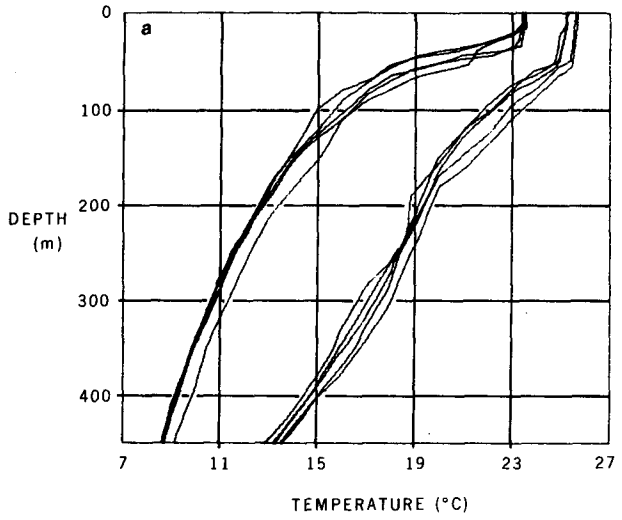

FIG. 2a. XBT profiles from quiescent regions north and south of the Tasman Front. The high-temperature profiles are from leg KL of Fig. 1c between 155.4 and 156.3°E; the low-temperature profiles are from the leg along 36°S in Fig. 1d between 155 and 156.2°E.

example, the northward branch across 33 and 34°S at 159°E in Fig. 1d had GEK currents up to 1 m s^{-1}; near H and J in Fig. 1c the GEK currents were 1.5 and 0.75 m s^{-1}, respectively, in the directions of the cyclonic isobars. These values are typical of the extreme currents encountered at the Tasman Front. Geostrophic currents calculated from the height-contour spacings in Fig. 1 lie in the same range from ~0.5–1.5 m s^{-1}.

The following approximate volume transports are based on Andrews's (1979) universal velocity profile for the area. This profile allows geostrophic velocity profiles to be extrapolated to great depths. He found that actual current profiles attain a vertical asymptote at ~2700 m depth, but we will adhere to the historical convention of calculating baroclinic transports over the uppermost 1300 db. Accordingly the volume transport V (m^3 s^{-1}) is related to the change in dynamic height ΔD (0/1300), [geodynamic meters (gdm)] between two stations by

$$V = 28 \times 10^6 \Delta D/\sin(\text{latitude}). \quad (2)$$

At latitudes near Sydney this is ~50×10^6 m^3 s^{-1} for each meter change in dynamic height.

Applying this analysis to Figs. 1a–1c we find the southward transport between Coffs Harbour and Sydney has a representative figure of 35×10^6 m^3 s^{-1}. This stream then turns eastward and, from Figs. 1a, 1b and 1d, we find that the volume flow in the Tasman Front after leaving the continental shelf is about the same. At first glance one might be tempted to say that the Front carries ~35×10^6 m^3 s^{-1} into the central Tasman Sea. In fact, volume transports of beyond 30×10^6 m^3 s^{-1} are associated with eddies adjacent to the Front which recirculate a large fraction of the water and do not allow it to progress continuously eastward. The net eastward transport is estimated from the averaged change in surface dynamic height anomaly in crossing the band occupied by the Front and its associated eddies. Very roughly, this is about 30 gdcm so the net zonal transport is ~15×10^6 m^3 s^{-1}; Stanton (1976) found the transport in the Front within the square on Fig. 1a ranged from 10×10^6 to 14×10^6 m^3 s^{-1}.

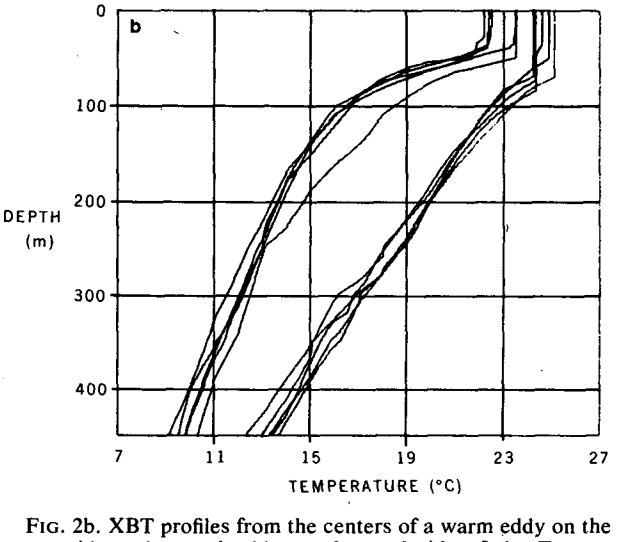

FIG. 2b. XBT profiles from the centers of a warm eddy on the warm side and a cool eddy on the cool side of the Tasman Front. The profiles are from the leg along 34°S in Fig. 1d; the high-temperature profiles lie between 157.7 and 158.7°E, while the low-temperature profiles lie between 159.6 and 160.5°E.

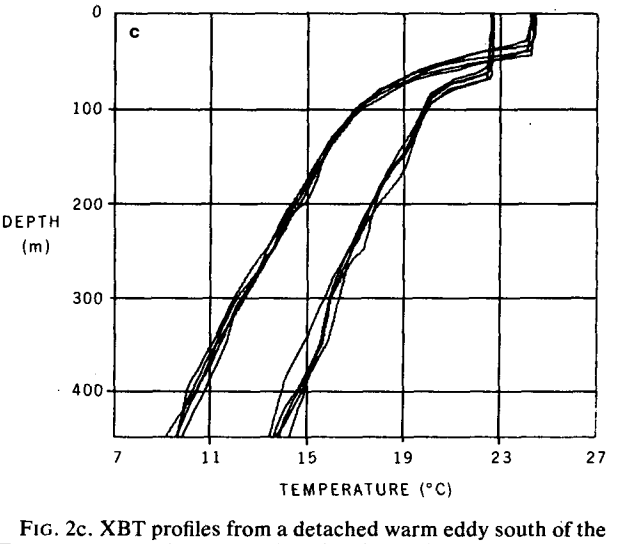

FIG. 2c. XBT profiles from a detached warm eddy south of the Tasman Front and a detached cool eddy north of the Front. The high-temperature profiles are from the leg along 36°S in Fig. 1d between 151.5 and 152.4°E; the low-temperature profiles are from leg HIJ of Fig. 1c, 50 km either side of I.

4. Water column integrity and thermocline shapes

In this section we discuss the difference between the shape of the thermocline in the South Coral and Tasman Seas generally and in particular we investigate whether the thermocline is modified near the Front.

Fig. 2a shows five XBT profiles from the South Coral Sea, well north of the Front, and five from the Tasman Sea, well south of the Front. The (warm) South Coral Sea profiles come from leg KL of Fig. 1c near 156°E while the (cool) Tasman Sea profiles come from Fig. 1d along 36°S between 155 and 156°E. We see that the essential difference between the two is that the thermocline is colder at all depths in the Tasman Sea with the maximum difference of ~6°C occurring over about 150–300 m depth. A slightly more subtle difference enables us to identify the origin of a water column: below the mixed layer, South Coral Sea profiles are very nearly linear while Tasman Sea profiles have a shallower, rounded, somewhat exponential thermocline down to ~200 m where the profile then becomes linear.

The two sets of profiles in Fig. 2a were taken from the same longitude but were ~1000 km apart in the north-south direction. Figure 2b contains five high-temperature profiles from near the center of the anticyclone at 34°S, 158.5°E in Fig. 1d and five low-temperature profiles from near the center of the cyclonic meander at 34°S, 160°E also in Fig. 1d. Thus Fig. 2b contains two classes of profiles only 140 km apart (with the nearest from the two classes only 80 km apart) and separated by the Tasman Front with the warm water on the South Coral Sea side and the cool water on the Tasman Sea side. The high-temperature profiles have the linear thermocline characteristic of the South Coral Sea, while the low-temperature profiles have the shallower, rounded thermocline nearer the surface, becoming linear beyond 200 m depth. Comparison of Figs. 2a and 2b shows that the water columns identifiable with either the Tasman or the South Coral Seas maintain their integrity even in the intense meandering regions near the Tasman Front. There is no significant difference between Figs. 2a and 2b and our experience not only with the data from these experiments but from the many surveys conducted in the western parts of the central Tasman and South Coral Seas convinces us that the shape and mean temperature of the profile is a valuable indicator of water type and origin in the upper levels in these areas. In fact, the Tasman Front is simply a sharp boundary between two bodies of water with different vertical temperature profiles. Currents are necessitated by the pressure change across the Front, and the required feed water comes from the East Australian Current. Hamon (1968a) noticed that a difference in dynamic height implied not only a change in vertically averaged temperature but also a change in thermocline shape, although the presence of the Tasman Front was not known at the time.

An obvious question now is "What are the shapes of temperature profiles in warm eddies south of the Front and in cold eddies north of the Front?". In Section 5 we show that the low-pressure cell in Fig. 1c centered at 32°S, 157.5°E is an isolated cyclonic eddy to the north of the Front; it is obvious from the height-contour pattern in Fig. 1d that the anticyclone centered at 36°S, 152°E is isolated and is south of the Front. Fig. 2c shows five high-temperature profiles from the center of the anticyclone and five low-temperature profiles from the center of the cyclone. Mixed-layer temperatures in Fig. 2c are transposed with those in Figs. 2a and 2b, an event which could have many causes. The important point is that below the surface layer the warm eddy has the linear thermocline typical of South Coral Sea water and the cool eddy has the shallow, rounded thermocline typical of the Tasman Sea. There has been some cooling of the thermocline in the warm eddy and some warming of the thermocline in the cool eddy, of ~1°C over the interval 100–450 m. This is presumably due to lateral, subsurface diffusion of heat into the cool eddy embedded in the warm South Coral Sea and out of the warm eddy embedded in the cool Tasman Sea in the manner discussed by Nilsson and Cresswell (1980). We conclude that when eddies detach from meanders of the Front, the thermoclines in the centers of the eddies largely maintain their integrity.

5. Meanders and isolated eddies

It is obvious from Fig. 1 that the position of the Tasman Front varies markedly in space and time by executing mesoscale, lateral meanders. These give the Front an appearance similar to the Gulf Stream after it leaves the coast to form an interface separating "slope water" from Sargasso Sea water; it is also quite like the Kuroshio-Oyashio front.

We now address the question of which of the meanders in Fig. 1 can properly be called closed eddies and which of the closed eddies can properly be regarded as detached from the main frontal system. The criterion we adopt for calling an eddy closed is that surrounding some central pressure anomaly there should be a series of closed dynamic-height-anomaly contours to represent a closed orbit for a circulating water particle; drifting buoy data (e.g., Nilsson and Cresswell, 1980) show that orbits coincide well with closed contours. According to this criterion a localized intensification within an elongated meander would be a closed eddy. We regard a closed eddy as detached if its water type

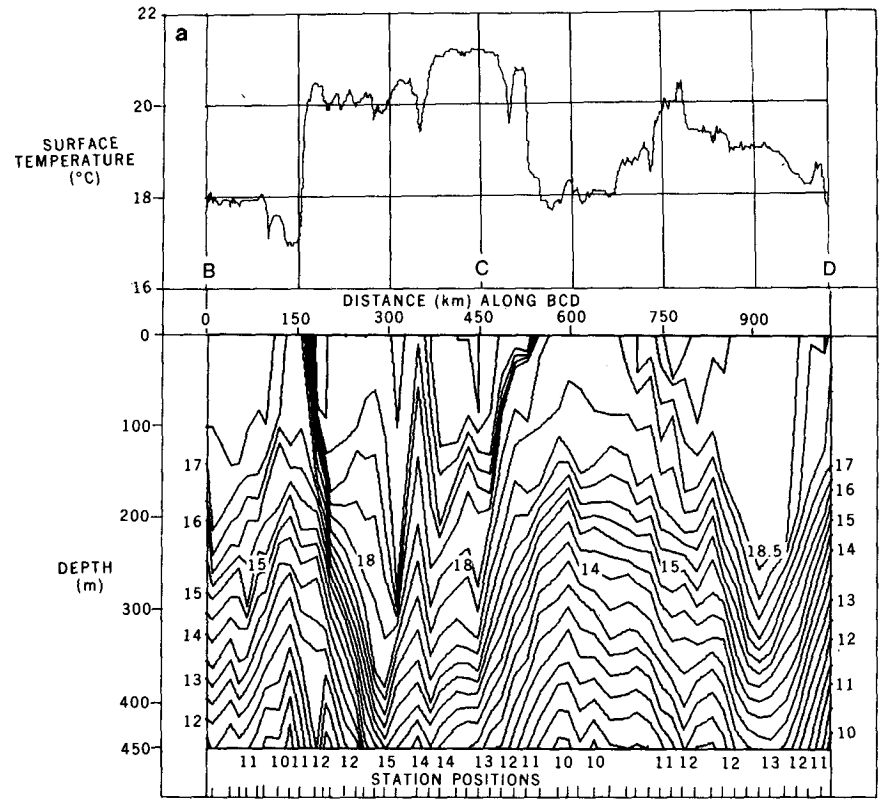

FIG. 3a. Temperature section (°C) from XBT probes and a thermograph sea-surface temperature trace along leg BCD of Fig. 1a.

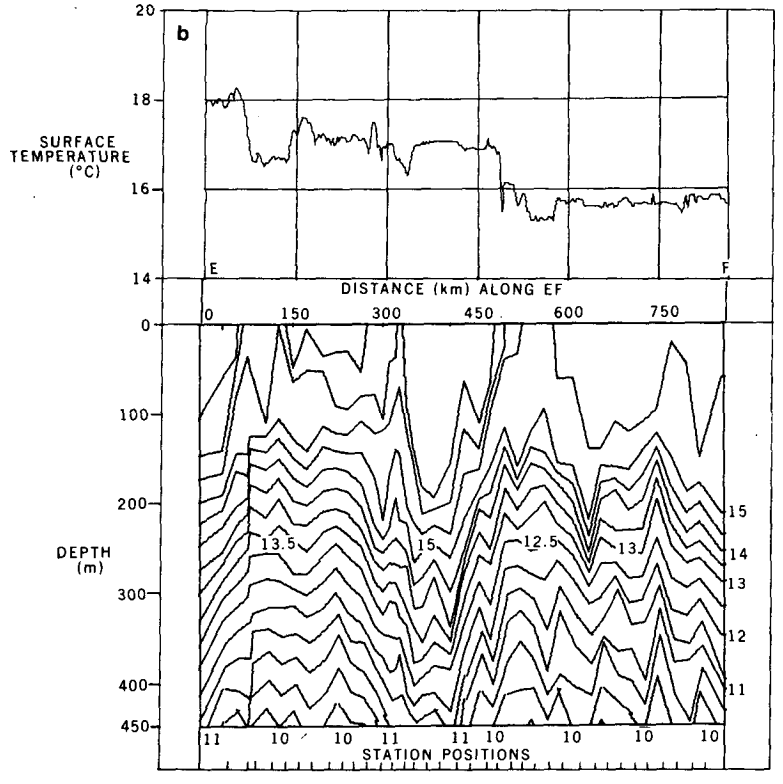

FIG. 3b. As in Fig. 3a except along leg EF.

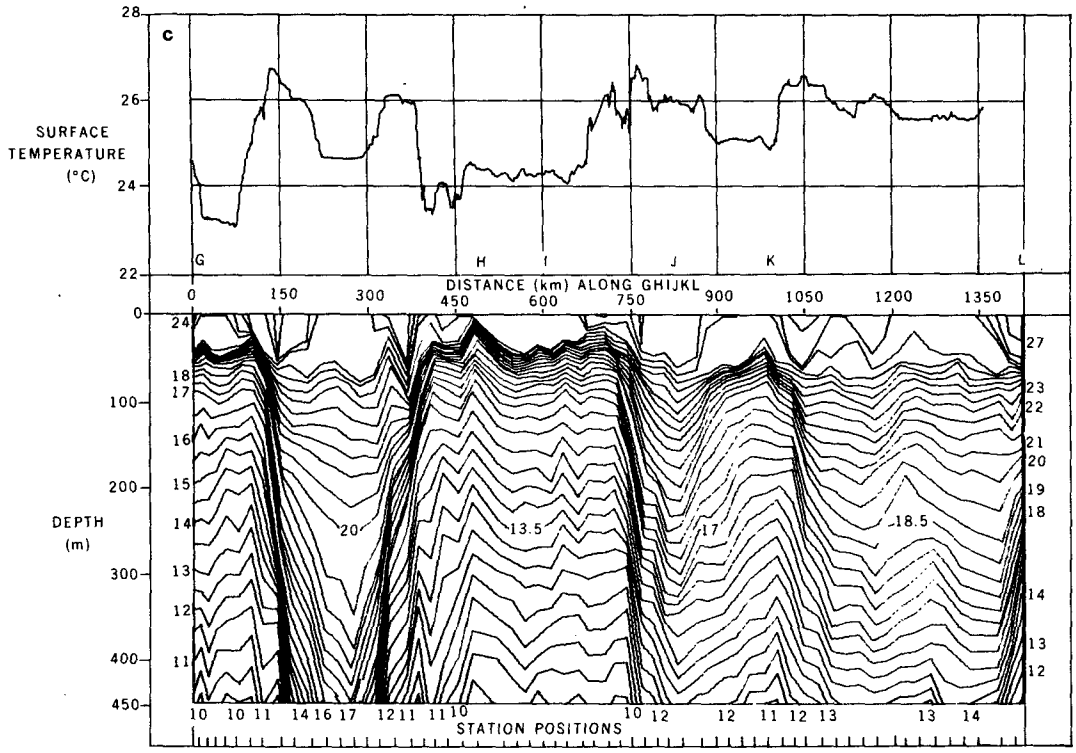

FIG. 3c. Temperature as in Fig. 3a except along leg GHIJKL.

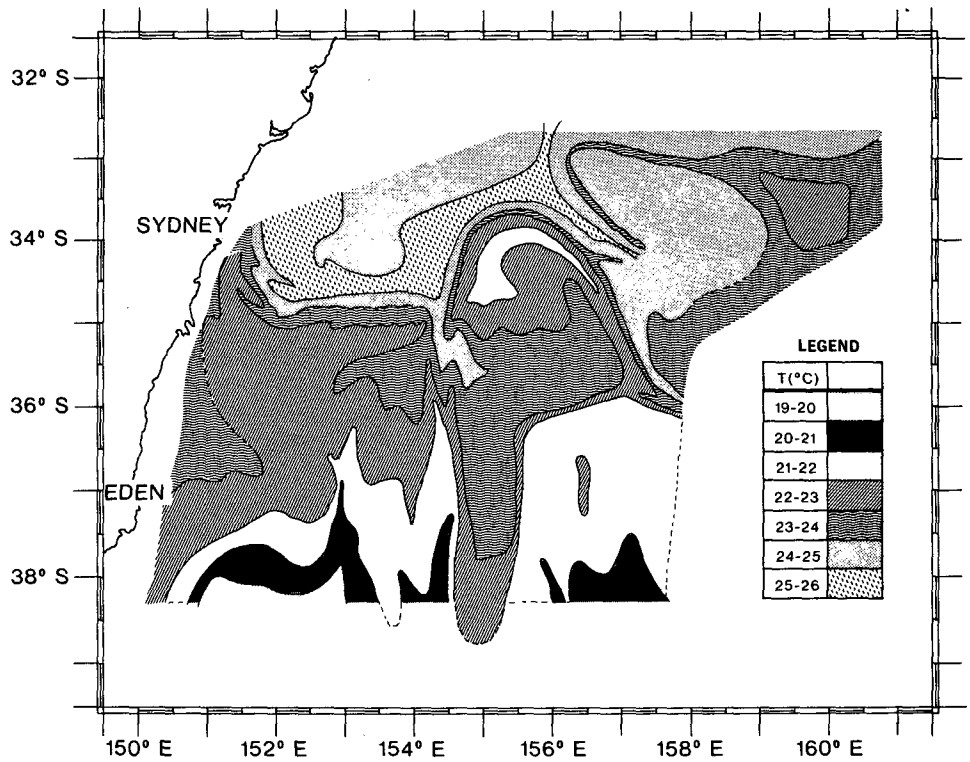

FIG. 4. Sea surface temperature patterns from thermograph along cruise track of Fig. 1d. Individual isotherms have been drawn and the regions between have been shaded to show 1°C resolution zones according to the legend.

is separated from the Sea of its origin (either South Coral in the case of warm core eddies or Tasman in the case of cool core eddies) by the Tasman Front. Obviously, a detached eddy originates in a meander which intensifies into a closed eddy; the final process is the reformation of the Tasman Front behind the breakaway entity.

The only data we have for experiment 2 are AXBT profiles and these are summarized in the dynamic topography in Fig. 1b. There is a warm southward meander near the coast and a cool northward meander east of this. As signified by the dashed lines, the sparsity of data at the top of the northward meander prevents any further interpretation of that eddy structure.

Fig. 1a provides some good examples of cyclonic and anticyclonic meanders which appear to have intensified to the point where they contain closed eddies. Fig. 3a shows the temperature section along the track BCD of Fig. 1a. We have anticyclones located at 32°S, 155°E and at 30.5°S, 160°E in Fig. 1a. The thermal structure of Fig. 3a shows that the first eddy contains anomalously warm surface water (20–21°C) and depressed isotherms in the thermocline between the distance marks of 150 and 500 km from B. The fronts are very abrupt at the surface, being only ~30 km wide, but are up to 120 km wide within the thermocline. The warm surface water (and indeed the whole thermocline) originates in the South Coral Sea. The second closed anticyclone (near 160°E) is seen as depressed isotherms between the distance marks of 800 and 1030 km on Fig. 3a and exhibits a typical anomalously deep and warm winter-mixed layer. The 20°C surface water shown at 750–800 km in Fig. 3a is South Coral Sea surface water advected south round the western edge by the eddy current.

There is a cyclonic meander at 30.5°S, 162°E in Fig. 1a which was fairly well delineated by AXBT's (filled circles), partial circumnavigation (cruise track), and a second visit by HMAS *Diamantina* (open circles). Tasman Sea surface water of ~18°C lay within the meander and the ship's course around DE was chosen in large part by a desire to criss-cross the surface temperature front. This meander contains closed orbits for water particles but intensification or eddy closure is very poorly developed when compared with, say, the two anticyclones just previously discussed.

We see the probable next stage of development, namely indications of the reformation of the Tasman Front behind a detaching feature, in the cyclonic eddy centered at 30.5°S, 158°E in Fig. 1a. The ship's track crossed this feature centered near the 600 km mark on Fig. 3a. This shows the elevation of the isotherms in the thermocline together with the 18°C surface water indicative of Tasman Sea water. There appears to be a swift eastward current south of this eddy along 33°S in Fig. 1a as well as the zonal cyclonic eddy current along 29.5°S. The dynamic height data are too sparse for us to state definitely that the Tasman Front was reforming south of the cyclonic eddy. However, surface mixed-layer temperatures show anomalously warm water drawn out along 33°S to 159.5°E and this reinforces the contoured interpretation we have put on the surface dynamic-height field of Fig. 1a.

The discussion now turns to eddies in the probable final stage of complete isolation from the Tasman Front. The literature contains many examples of detached anticyclones south of Sydney, adjacent to the Australian coast. Nilsson and Cresswell (1980) give a particularly full account of their evolution and even of anticyclone reabsorption by the Tasman Front. Fig. 1a shows one such typical high-pressure cell near 34.5°S, with Fig. 3a showing the vertical structure extending 120 km out from B, typical of a winter eddy. Fig. 1d shows a typical summer anticyclone south of the Front near 36°S. A trough separates the current ring in the south from the zonal jet in the north and it is worth noting that between 36 and 35°S the baroclinic surface dynamic-height anomaly falls 50 cm and then rises 100 cm between 35 and 34°S. There is another isolated anticyclone in the southeast corner of Fig. 1d. It is elliptical with a major axis parallel to the coastline and a dynamic-height relief, from center to edge, of only 15 cm. We know from the shapes of the XBT profiles that it originated from South Coral Sea water passing through the Front, but most of the excess heat has been lost from the thermocline and the central surface temperature anomaly is only slight (see Fig. 4).

The cyclonic eddy shown in Fig. 1c centered on 32°S, 157.5°E has temperature profiles shown in Fig. 2c which identify its origin as the Tasman Sea. Vertical structure in Fig. 3c shows the very strong fronts near the 400 and 750 km distance marks and a pool of anomalously cool surface water with a temperature near 24°C within the current loop. The data do not extend sufficiently far in the southeast corner of Fig. 1c to show whether the eddy was closed during the air and sea surveys of 8–19 February 1979. It was certainly closed and detached by the completion of the ship survey from 22 February–12 March 1979: the dynamic-height pattern for that survey (Fig. 1d) shows the Tasman Front reconstituted along latitude 34°S, thereby separating the water in the cyclonic eddy to the north from its Sea of origin. The changing position of the Tasman Front can be inferred by considering Figs. 1c and 1d jointly. The most reasonable explanation is that the main current flowed south past Coffs Harbour and Sydney (Fig. 1c), diverted seaward at ~34°S and northward along longitude 156°E, (Fig. 1d) then to flow around an elongated equatorward meander (Fig. 1c), which subsequently

pinched off while the main current reformed along latitude 34°S (Fig. 1d).

In summarizing this section we may say that eddies apparently are shed to the north and south of the Front as detached meanders. More particularly, warm eddies are detached to the south near the coast and one-half of a wavelength farther east cold eddies detach to the north, not necessarily in a dynamically linked fashion or simultaneously. The process may repeat itself with the next sort being warm eddies at one full wavelength, and so on. Finally, although we have put the most plausible (or so it seems to us) interpretation on our data we must emphasize that since we do not have the necessary time series of observations, the precise details of the steps involved in separation of eddies have yet to be conclusively defined.

6. Surface temperature

In this section the relationship between sea surface temperature and the baroclinic structure of the Front and its eddies is examined, particularly with a view to deciding whether the position of the Front can be monitored remotely (e.g., from satellites). We already know that newly formed winter anticyclones have warm anomalies within their current rings and that both summer and winter anticyclones have tongues of warm northern water advected round the forming eddies (Andrews and Scully-Power, 1976; Nilsson *et al.*, 1977; Andrews, 1979). These older data were taken within one-half wavelength of the Australian coast; the present data allow an analysis of cold core cyclones and also warm core anticyclones over a much larger area in both summer and in winter. The winter experimental data from 29 August–11 September 1978 are shown in Fig. 1a and in Figs. 3a and 3b. On proceeding north along BC the surface temperature (Fig. 3a) fell from 18 to 17°C. The fall marks the passage into the trough separating the high-pressure cell (at B on Fig. 1a) from the Tasman Front to the north. When the Front was crossed near the 150 km mark on Fig. 3a the surface temperature rose ~4°C at a maximum rate of 3°C over 6 km. The surface temperature north of the Front, within the high-pressure cell near C on Fig. 1a, stayed ~3°C higher than that of the Tasman Sea surface water immediately south of the Front (near B, or 18°C). About 75 km along CD (near the 525 km mark) the surface temperature fell, just as abruptly as it had risen, back to ~18°C, to mark entry into the almost detached cyclonic eddy. This eddy is marked by the elevated isotherms in Fig. 3a and is bounded to the south by the dynamic-height contours and the warm mixed-layer water extruding along 32.5°S in Fig. 1a. The cool surface water in the cyclonic eddy then merged fairly slowly with a warm peak near the 750 km mark on Fig. 3a; the vertical isotherm section shows that the peak, with a temperature near 20°C marks the transition from the cyclone to the anticyclone northeast of Lord Howe Island in Fig. 1a. The anticyclone contains surface water ~1°C warmer than that near B. Fig. 3a breaks off where the surface temperature fell as the anticyclone's eastern edge was crossed and partial circumnavigation of the cold feature near 162°E on Fig. 1a began.

We have described a sequence of warm and cold patches of surface water associated with cyclonic and anticyclonic eddies near and in the Tasman Front in winter. The story continues across the Tasman Sea with Fig. 3b, which has a different sort of thermal signature from that in Fig. 3a. There is a continual trend of falling surface temperature along EF. The slopes of the isotherms and the coherence of the wavy structure in the thermocline also decline along EF. The data in Fig. 1a from the eastern Tasman Sea are too sparse to allow us to draw many conclusions about the nature of the Tasman Front there, except to say that we think the track EF only cuts across the southern portion of the meander pattern.

One might expect the ocean currents in summer, when surface warming occurs, to be obscured in the sense that the surface temperature signature of deeper baroclinic events might be obscured by surface warming and so be undetectable from ships or satellites. The data from experiments three (8–19 February 1979) and four (22 February–12 March 1979) show that this is not the case, and surface temperatures reveal the position of the East Australian Current and the Tasman Front just as clearly in summer as they do in winter.

Surface temperatures are displayed in different fashions for experiments three and four in Figs. 3c and 4. Since the data were gathered over a month, Figs. 3c and 4 should not necessarily be expected to match in more than a qualitative fashion. There is an obvious overall fall of surface temperature from north to south of ~6°C in about 1000 km; however, near 28°S, on leg KL of Figs. 1c and 3c, we have the northernmost data and the highest temperatures near 26°C, while the southernmost leg of Fig. 4 has temperatures near 20°C.

The cruise track GHIJKL cuts into the poleward meander on Fig. 3c ~150 km from G. The strong front in the thermocline shows the southward baroclinic current which advects warm water from northern latitudes. The surface temperature peaks near the 150 km mark at ~26.5°C, so it has obviously been carried south from the latitude of Brisbane. This was confirmed by measurements made while HMAS *Kimbla* returned from Brisbane to Sydney during 24–27 February 1979: the GEK showed that a current from 3–4 kt flowed south

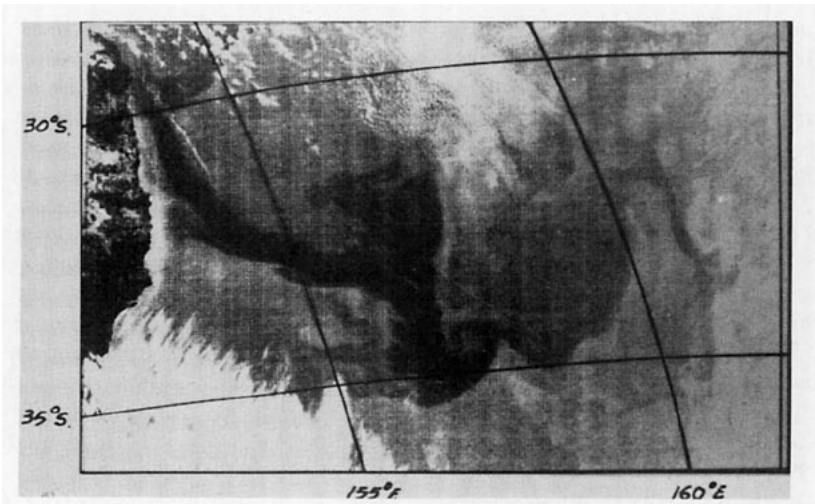

FIG. 5. Digitally enhanced sea surface temperature image of NOAA-4 infrared surface photograph for 13 September 77. Dark areas indicate warm water.

from Brisbane to Coffs Harbour and then west of south from Coffs Harbour to Sydney where it joined the Front depicted in Fig. 1d. Surface temperature peaked near 26°C where the current was strongest and fell off by ~1°C on the seaward side of the southward flow. This behavior is seen in Fig. 3c where the temperature falls toward the center of the ridge near the 225 km mark. Farther along the track the surface temperature climbs back to a peak of 26°C at the position of the northward baroclinic current on the eastern side of the poleward meander near the 350 km mark. The cooler surface water near 24°C, residing within the cyclonic current ring, lies between the 375 and 675 km marks. Once again, as the baroclinic current intensifies, the surface temperature rises to peak near 26°C at the 750 km mark. We have therefore traced warm northern water advected on the strong currents shown in Fig. 1c south from Brisbane, around the poleward meander near Sydney, and then north and east around the cyclonic eddy centered on 157.5°E. This warm stream has a temperature from 1–4°C higher than adjacent surface water.

The final summer surface temperature data discussed in this paper are those for experiment 4 (Fig. 4) which may be correlated with the dynamic-height pattern of Fig. 1d. One notes immediately the extrusion of very warm (>25°C) surface water along the 190 dyn. cm contour representing the Front near 34°S; this feature thins and splits near 155.5°E into a northward branch around the high in Fig. 1d and a southeastward branch along the Front. This hot water advected from the north is only one of the two sea surface temperature markers which show the position of the Front. The second identifying marker is the sharp horizontal temperature gradient that lies just south of the band of 25–26°C water out to 156°E, and then marks the southeastward stream in Fig. 4. The distortion of isothermal surfaces in the thermocline has been shown to be most marked near the Tasman Front and there is an instance here where we are persuaded that deep-sea upwelling occurred. We believe this produced the crescent of relatively cool 21–22°C water near 34°S, 155°E in Fig. 4. The temperature section (not shown here) from the cruise track cutting the Tasman Front shows a wedge of cool water rising from ~120 m depth north of the 190 gdcm height contour to surface south of the Front.

Careful comparison of Figs. 4 and 1d shows other correlations mainly in the form of pooling of isothermal water near centers of dynamic height anomaly and stretching of surface isotherms along regions of strong geostrophic currents. Without the benefit of hindsight supplied by Fig. 1d these correlations, far from the Front, could not be automatically forecast with confidence. One can be reasonably confident however that sea surface temperature patterns near the East Australian Current and the Tasman Front can be interpreted usefully in terms of flow.

7. Some satellite observations

In this section we present two satellite infrared photographs of areas in the Tasman Sea in which oceanographic data were taken from surface vessels simultaneously, thereby allowing comparisons to be made. We are seeking to show that the surface temperature effects observed from ships can also be observed remotely, from satellites.

Fig. 5 is a NOAA-4, VHRR photograph taken on 13 October 1977. HMAS *Diamantina* was steaming in consort with HMNZS *Tui* from Brisbane to the site of an acoustic experiment east of Sydney near that time. Ship thermograph and XBT data

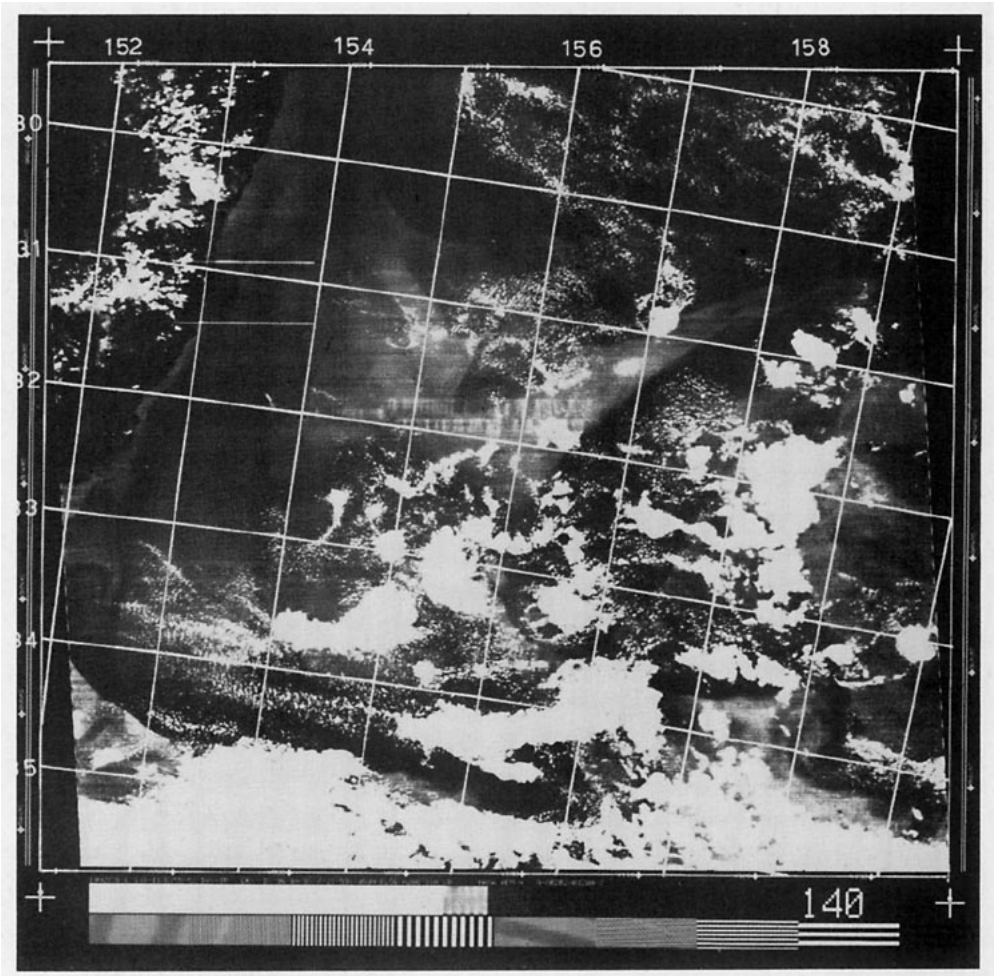

FIG. 6. Photographically enhanced sea surface temperature pattern from the HCMM infrared surface photograph for 14 November 78. Dark areas indicate warm water.

show that the warm plume in Fig. 5 along 153.5°E north of 32°S marks the East Australian Current, with a surface temperature higher than the flanking water by 2 to 2.5°C, the plume being advected by a geostrophic current increasing from 70 cm s^{-1} at 30°S to 150 cm s^{-1} at 32°S. Ship XBT data also confirm that the current left the coast at 31.5°S to become a zonal stream crossing 154°E at 32°S. Fig. 5 shows that near 156.5°E the zonal stream bifurcated to form one segment heading north with a warm branch centered on 156.5°E and one segment heading south and then east, disappearing at ~157.5°E. The northward branch may be linked to the topography as suggested by the numerical study of Godfrey and Robinson (1971); the edge of the Tasman abyssal plain has seamounts along 156°E between 30 and 34°S, while in broader terms the edge of the Tasman abyssal plain lies roughly parallel to the Australian coast between 26 and 34°S. The bifurcation is quite like that shown in Fig. 1d, and also the termination of the warm plume in the southward and eastward branch near 157.5°E on Fig. 5 is quite like the termination of the 25–26°C water near 156–157°E in Fig. 4. Notice that further east in Fig. 4, the Front is then marked by a straightforward surface-temperature gradient. If similar behavior applies in Fig. 5, then the Front is visible out to 161°E along the interface between South Coral and Tasman Sea surface water. If we accept this, then we can postulate that the cold water forms an equatorward (cyclonic) meander with a trough lying along the line 35°S, 160°E to 32°S, 160.5°E.

Fig. 6 is a HCMM (Heat Capacity Mapping Mission) infrared photograph for 14 November 1978 and the interpretation is far less straightforward than for Fig. 5. We rely on some CSIRO cruise results (RV *Sprightly* cruises SP 15/78, 17–29 November 1978; SP 17/78, 9–11 December 1978) for a preliminary description, although these data were taken only within 100 km of the coast. The *Sprightly* data show that the East Australian Current flowed south between 27 and 29°S along the coast at speeds of ~1 m s^{-1}; the current then left the coast at

29.5°S and diverted to the southeast. This explains the origin of the thermal front on Fig. 6 entering the top of the picture at 154°E. This front converged with the coastline at 28.5°S (off the photograph), as observed from RV *Sprightly* on 24–25 November 1978. We see in Fig. 6 that this branch of the current continued seaward across 155°E at 30.5°S, and then the front meandered eastward between 30 and 31°S. South of this thermal front there was a very large pool of cool surface water centered near 31.5°S, 155°E. A filament of this surface water was carried to the northeast across 31°S, 157°E and beyond, where one can see billows as if the filament was contorted by a shear current. To the west of the pool of cool water, there was a thin stream of warm water along the coast from 29.5°S to Sugarloaf Point (32.5°S) and continuing southward to 34°S where it blended with an intense eastward front. The data from SP 15/78 and SP 17/78 show there was a southeastward-to-eastward flowing jet near 34°S, 152°E fed by (and lying between) a cyclonic disturbance to the south and an anticyclonic disturbance to the north. In Fig. 6 we see what we call the Tasman Front between 34 and 35°S as far east as 157°E, where cloud cover obscures the picture. Finally, there was a cool equatorward intrusion of Tasman Sea water between the eastern edge of the photograph and ~158°E, extending north to 31°S.

Apparently, the East Australian Current system was split into two eastward meandering components. One component left the coast near 28.5°S to meander east along 30–31°S while the Tasman Front lay between 34 and 35°S, then to meander north around the cyclonic intrusion. It is reasonable to assume that these two branches joined at the nose of the intrusion to flow across 159°E near 30–31°S. It is instructive to compare Figs. 6 and 1b, which show data taken four weeks apart. The main feature of the Tasman Front in mid-November (Fig. 6) is still present in mid-December (Fig. 1b); in Fig. 1b the Front leaves the coast near 34°S and then meanders north around a cyclonic intrusion, as it did in mid-November.

In this section we have seen that a satellite study of the Tasman Front will be valuable and that there are two key features to be seen from space which can be easily associated with the Front: one is very warm northern water advected south along the path of the current and the other is the inherent difference in temperature between surface waters of South Coral and Tasman Sea origin near the Front.

8. Scales of the motion and linearity

The zonal wavelength of the meander patterns in Figs. 1 can be determined easily by eye and is ~370 km, with not much variation between the four experiments. This is in good agreement with determinations made from structure function analyses (Andrews, 1979). We now consider propagation speeds and the linearity of an internal baroclinic wave model for these meanders.

Assume the baroclinic pressure anomaly is given by

$$y = y_0 \exp[i(kx + ly + \omega t)], \tag{3}$$

where y_0 is the amplitude, $k = 2\pi/370$ km $= 1.7 \times 10^{-5}$ m^{-1}, and ω is the angular frequency. If we use Lighthill's (1969) normal mode theory, and the observation that k is much larger than l, the classical dispersion relation for the first internal mode is

$$\omega = -\beta k/(k^2 + 1/\mu^2), \tag{4a}$$

where

$$\mu = (gH_1/f^2)^{1/2} \tag{4b}$$

is the Rossby radius of deformation, H_1 the eigendepth for the first mode, and f the Coriolis parameter, with a gradient of β. Andrews (1979) has computed the eigendepth off Sydney, $H_1 = 79$ cm, so the Rossby radius of deformation is $\mu = 33.4$ km at latitude 35°S. The ratio of the wavelength of the meanders of the Tasman Front to deformation scale meanders, therefore, is $1/k\mu = 1.8$. The phase speed

$$c_p = \omega/k = -\beta/(k^2 + 1/\mu^2) \tag{5a}$$

is 1.6 cm s^{-1} westward, while the group velocity

$$c_g = \partial\omega/\partial k = c_p(1 - (\mu k)^2)/[1 + (\mu k)^2] \tag{5b}$$

is 0.8 cm s^{-1} westward. These phase and group velocities of ~1.4 and 0.7 km day^{-1} are an order of magnitude smaller than the speeds at which fronts are generally observed to move, albeit sporadically; and the time scale $T = 370$ km$/c_p = 9$ months is an order of magnitude too large. Hamon (1962, 1968b) found a period more like 20–50 days, while Hamon *et al.* (1975) found that fronts, or current patterns, move at ~9 km day^{-1}. Indeed, the front near J on Fig. 1c moved south at 15 km day^{-1} during the four days between the aircraft survey and the crossing by HMAS *Kimbla* while, similarly, the front near H moved west at ~20 km day^{-1}.

We cannot then look to linear theory to explain observed rates of change. Nonlinear processes transfer energy between wavenumbers by causing small eddies to cluster into ordered, deformation-scale motion, or by destabilizing large length-scale planetary waves and zonal flows. Rhines (1973, 1977) uses the wave steepness ϵ as a measure of the importance of these nonlinear processes. In the present case steepness is calculated from the ratio of the field accelerations to the local accelerations, i.e.,

$$\epsilon = U_i \frac{\partial u_j}{\partial x_i} \Big/ \frac{\partial u_j}{\partial t}, \tag{6}$$

where U and u may belong to different spectral components and the i and j directions may be different. Repeated indices do not imply summation. For a zonal, meandering current we should investigate u_j = northward geostrophic current and x_i = eastward distance, whereupon Eqs. (6), (3) and (4) give

$$\epsilon = Uk/\omega = U(k^2 + 1/\mu^2)/\beta. \quad (7)$$

Here U is the rms depth-averaged velocity associated with the zonal flow.

We know that separated eddies in the East Australian Current system originate from a system with a wavelength of 1.8 times the deformation-scale wavelength and we know that, on separating, they become deformation-scale eddies (Andrews and Scully-Power, 1976; Andrews, 1979); thus we might *a priori* expect wave steepness of order unity or greater. The averaged drop in surface dynamic-height anomaly across the Front was earlier noted to be ~30 cm; and the eddies and meanders disperse this across a zone up to, at most, 600 or 700 km wide, so a scale for U from the geostrophic relation and the shapes of current profiles (Andrews, 1979) is ~2 cm s^{-1}. Using this value in Eq. (7), we find ϵ is ~1.25 and we conclude that nonlinear processes are important in any dynamical interpretation of the Tasman Front.

To recapitulate, the ratio of the length scale of the meander pattern to the natural length scale (Rossby radius of deformation) is 1.8 so that it is only after the eddies detach from the Front that they assume the natural length scale. Second, the steepness of the wave pattern is ~1.25 so the frontal dynamics are nonlinear; in simple terms it seems that the effect of the meanders is to disperse the dynamic-height change sufficiently broadly that the nonlinear influence is kept within reasonable bounds.

9. Discussion

It seems clear that a zonal band ~600 km wide centered near 33 or 34°S contains a meandering front stretching from Australia to New Zealand. Prior to our experiments, one could have expected this to be the case for a number of reasons. First, time- and space-averaged maps of dynamic height in the southwest Pacific show a broad zonal flow (e.g., Reid, 1961; but notably Wyrtki 1962, 1974) which passes north of New Zealand. Second, spatial fluctuations appear in single-cruise data from these latitudes when they have not been averaged; we have two complete temperature sections across the Tasman Sea between Sydney and North Island (20–25 March 1976 and 3–7 April 1978; not presented here) which show essentially the same behavior as Figs. 3a and 3b. Furthermore, we have a temperature section (4–7 September 1978) from Bass Strait to the North Cape of North Island which does not show significant fluctuations. Thus there seemed to us to be a southern limit to the area where eddies are formed. The possibility of the existence of a northern limit as well, and to us therefore of a zonal band, was established by CSIRO in 1960 (Anon, 1962). They occupied a section along latitude 34°S from Sydney to New Zealand (3–8 February 1960), which showed typical eddy fluctuations, and a similar section along 30°S from Australia to 170°E (18–22 March 1960) wherein there were no regular eddy fluctuations.

These historical data were fragmentary and only presented a case for conducting the present investigation. If we couple the historical data with those given here and with Stanton's (1976) investigation, however, there is no doubt that the Tasman Front is a permanent feature joining the East Australian Current across the northern tip of North Island (presumably) into the southern limb of the South Pacific subtropical gyre. Thus our faith in the integrity of the East Australian Current is restored; if an observer stands on the Australian coast near Coffs Harbour he will see a southward current at times near the coast (Fig. 1c) and at times farther out to sea (Fig. 1a). It appears from present and historical data that the current will rarely cross the Tasman Sea after leaving the coast farther north. Whichever the case, it seems likely to us that a complex meandering system will always be found through which a western boundary current threads its way into the Tasman Front. It is the complexity of the meanders which led Hamon and Tranter (1971) to question the significance of the East Australian Current in the total circulation in the western South Pacific.

Warren's (1970) arguments are now very compelling. Essentially, he took Welander's (1959) Sverdrup solution, which ignored the meridional barrier posed by New Zealand, and pondered the most likely real effect of New Zealand on that solution: Welander's interior solution across the portion of the South Pacific between New Zealand and South America would require a supply of water to the equatorward flow from a western boundary current at the partial barrier (New Zealand). This in turn must be fed from the Tasman Sea west of New Zealand; but since any meridional velocities there are fixed by local wind-stress curl, the only connecting flow can be zonal. This in turn implies that the East Australian Current must leave the Australian coast at the latitude of the North Cape of North Island (34°S) where a zonal flow is required to supply the New Zealand western boundary current. We conclude that topography (New Zealand) and wind stress (the Sverdrup solution) play the dominant role in establishing the Tasman Front observed by us and others. This has been a brief presentation of Warren's argument, which

suffered from deficiencies in the wind-stress data and the spatial scale (5° squares) used by Welander (1959), and from excluding the effects of both stratification and bottom topography.

Cox (1975) was able to quantify Warren's (1970) arguments by using a 2° grid with Hellerman's (1967) improved annual-mean wind-stress field. Although he ran a full numerical model of the world ocean he paid particular attention to the circulation in the South Pacific and he used Warren's paper as a framework for discussing the circulation there. His first experiment with a homogeneous ocean reproduced neither the East Australian Current nor the Tasman Front because of effects of bottom topography. In his second experiment he used the observed averaged stratification and constrained it to be invariant with time. The result was the same; no Current and no Front developed west of New Zealand. He started his third experiment with the same averaged stratification but allowed it to change with time, i.e., he allowed baroclinic adjustment to evolve. In this case a broad East Australian Current developed transporting 22×10^6 m^3 s^{-1} southward, all of which abruptly turned eastward as a zonal flow at the latitude of the North Cape of North Island and continued as a western boundary current along the east coast of New Zealand. This set of three numerical experiments strongly suggests the following roles for wind stress, topography and stratification: the curl of the wind stress produces a basic Sverdrup circulation in the interior, which is qualitatively and quantitatively adequate as a first approximation for the time-averaged transport so long as baroclinic adjustment reduces the effect of bottom topography to something negligible. New Zealand and Australia form the western meridional barrier along which must flow the western boundary current required to close the interior solution. A zonal flow (the Tasman Front) is required across the Tasman Sea to connect the two separated boundary currents; the baroclinic character of this flow is responsible for differences like those in Fig. 2. Thus we may say that the difference in density structure (i.e., the Tasman Front) is maintained essentially by the wind-driven circulation in the central and eastern South Pacific Ocean and the split western boundary.

This is the circulation picture on time and space scales which exclude eddying mesoscale motion. In discussing these smaller scales we would have to consider the creation and intensification of meanders in a zonal baroclinic flow over topography. It is fairly clear now that wind stress is important only insofar as it sets up the interior circulation over the South Pacific Ocean, and does not play a primary role in the creation of meanders. We find that we cannot progress much beyond simple scale arguments and these merely show that both baroclinic and topographic processes can be important. The exclusivity of poleward meanders near the Australian continental separation point simply results from the poleward flowing coastal current being forced to flow eastward near latitude 34°S, and this exclusivity is probably aided by the peculiar channel like topography described in Section 7. We would also expect the currents to meander on crossing the Lord Howe Rise and the Norfolk Ridge. Even in a flat-bottomed ocean, the wave steepness is sufficiently large that eddy formation, as simulated numerically by Rhines (1977), must occur. There are sufficient observational data now to investigate the relative effects of the bottom and baroclinic adjustment in this region of the western South Pacific by constructing a baroclinic-barotropic-topographic numerical model.

A potential tool for monitoring the currents and eddies exists with satellite photographs. The two thermal effects, advected warm northern water and a horizontal jump in temperature across the Front, are associated with a baroclinic front in the thermocline and swift geostrophic currents. It should be possible to obtain valuable satellite time-series data on the positions of the thermocline fronts through the correlation between surface and deep structure; the major drawback is the extreme cloudiness of the area. We shall know more about the possibilities of infrared monitoring at the conclusion of the HCMM investigation.

We have given only approximate figures for current speeds and volume transports because we were interested principally in demonstrating that the continuous or time-averaged flow from Australia into the subtropical South Pacific gyre is only about half the figure generally assumed. It is usual to take a compilation of volume transport calculations and treat them statistically to obtain a figure for the mean transport; typically, then, for the East Australian Current one arrives at a figure of between 20 and 40 $\times$ 10^6 m^3 s^{-1}, for a reference level of 1300 db, from 35 individual transport calculations (see Andrews, 1979). Our data show that the larger transport calculations are associated with eddies near the Tasman Front which recirculate a lot of the water and a more realistic figure for the trans-Tasman transport is 15×10^6 m^3 s^{-1}. This figure is small compared with transports in other western boundary currents and with what is expected for the western South Pacific. It seems quite possible therefore that there are other contributions to the subtropical gyral transport southward from flows along meridional barriers like the Lord Howe Rise and the Norfolk and Kermadec Ridges.

Acknowledgments. This work is a contribution to the Australian Defence Science and Technology Organisation's project DST 78/071 and the National

Aeronautics and Space Administration's project HCM-051, the Heat Capacity Mapping Mission. Data were collected at sea from HMAS *Diamantina* and HMAS *Kimbla* and from the air by Orion aircraft of 11 Squadron, 92 Wing based at RAAF Edinburgh. The AXBT surveys were supported by the U.S. Office of Naval Research and we wish particularly to thank Dr. R. E. Stevenson for his support. Mrs. S. M. Ball and Mr. R. Schenk are thanked for their computing analyses. Dr. D. G. Nichol produced the digitally enhanced NOAA-4 infrared photograph.

REFERENCES

Andrews, J. C., 1976: The bathythermograph as a tool in gathering synoptic thermohaline data. *Aust. J. Mar. Freshwater Res.*, **27**, 405–415.

——, 1979: Eddy structure and the West and East Australian Currents. Flinders Institute for Atmospheric and Marine Sciences, Research Rep. 30, 172 pp.

——, and P. D. Scully-Power, 1976: The structure of an East Australian Current anticyclonic eddy. *J. Phys. Oceanogr.*, **6**, 756–765.

Anonymous, 1962: Oceanographical Investigations in the Pacific Ocean in 1960. CSIRO Division of Fisheries and Oceanography, Oceanographical Cruise Rep. No. 5, 255 pp.

Cox, M. D., 1975: A baroclinic numerical model of the world ocean: preliminary results. *Numerical Models of Ocean Circulation*, U.S. Nat. Acad. Sci., 107–120.

Denham, R. N., and F. J. Crook, 1976: The Tasman Front. *N.Z.J. Mar. Freshwater Res.*, **10**, 15–30.

Godfrey, J. S., and A. R. Robinson, 1971: The East Australian Current as a free inertial jet. *J. Mar. Res.*, **29**, 256–280.

Hamon, B. V., 1962: The spectrums of mean sea level at Sydney, Coffs Harbour and Lord Howe Island. *J. Geophys. Res.*, **67**, 5147–5155.

——, 1968a: Temperature structure in the upper 250 metres in the East Australian Current area. *Aust. J. Mar. Freshwater Res.*, **19**, 91–99.

——, 1968b: Spectrum of sea level at Lord Howe Island in relation to circulation. *J. Geophys. Res.*, **73**, 6925–6927.

——, and D. J. Tranter, 1971: The East Australian Current. *Aust. Nat. Hist.*, **17**, 129–133.

——, J. S. Godfrey and M. A. Greig, 1975: Relation between mean sea level, current and wind stress on the east coast of Australia. *Aust. J. Mar. Freshwater Res.*, **26**, 389–403.

Hellerman, S., 1967: An updated estimate of the wind stress on the world ocean. *Mon. Wea. Rev.*, **95**, 607–626 (Corrigendum, *Mon. Wea. Rev.*, **96**, 63–74).

Lighthill, M. J., 1969: Dynamic response of the Indian Ocean to onset of the southwest monsoon. *Phil. Trans. Roy. Soc. London*, **265**, 45–92.

Nilsson, C. S., and G. R. Creswell, 1980: Formation and evolution of east Australian eddies. *Progress in Oceanography* (in press).

——, J. C. Andrews and P. D. Scully-Power, 1977: Observations of eddy formation off east Australia. *J. Phys. Oceanogr.*, **7**, 659–669.

Reid, J. L. Jr., 1961: On the geostrophic flow at the surface of the Pacific Ocean with respect to the 1000 decibar surface. *Tellus*, **13**, 489–502.

Rhines, P. B., 1973: Observations of the energy-containing eddies and theoretical models of waves and turbulence. *Bound.-Layer Meteor.*, **4**, 345–360.

——, 1977: The dynamics of unsteady currents. *The Sea: Ideas and Observations on Progress in the Study of the Seas*, Vol. 6, *Marine Modeling*, E. D. Goldberg, I. N. McCave, J. J. Obrien and J. H. Steele, Eds., Wiley, 189–318.

Stanton, B. R., 1975: Vertical structure in the mid-Tasman Convergence Zone. *N. Z. J. Mar. Freshwater Res.*, **9**, 63–74.

——, 1976: An oceanic frontal jet near the Norfolk Ridge northwest of New Zealand. *Deep-Sea Res.*, **23**, 821–829.

Warren, B. A., 1970: General circulation of the South Pacific. *Scientific Exploration of the South Pacific*, Warren S. Wooster, Ed., U.S. Nat. Acad. Sci., 33–49.

Welander, P., 1959: On the vertically integrated mass transport in the oceans. *The Atmosphere and the Sea in Motion*, B. Bolin, Ed., Rockefeller Institute Press and Oxford University Press, 95–101.

Wyrtki, K., 1962: Geopotential topographies and associated circulation in the western South Pacific Ocean. *Aust. J. Mar. Freshwater Res.*, **13**, 89–105.

——, 1974: The dynamic topography of the Pacific Ocean and its fluctuations. Hawaii Institute of Geophysics, Rep. HIG-74-5, 19 pp.